Single Phase Immersion Cooling Solution for EV Batteries

Parth Sandip Patil, Sarvesh Suhas Patil, Bharathwaj Ramanathan,
Richard Manuel Menendez, Shreyan Milind Shastri, Shourya Sahdev.

University of Illinois Urbana Champaign, Department of Mechanical Science & Engineering,
1206 W Green St. Illinois, USA

Abstract

With accelerating climate change, reducing greenhouse gas emissions is critical. Electric Vehicles (EVs), a cleaner alternative to combustion engines, are pivotal in mitigating carbon footprints. EV batteries, the heart of the vehicle, dissipate significant heat—up to 1–5 kW for a 100 kWh battery during fast charging or acceleration. As the demand for faster EVs and longer-lasting batteries grows, efficient thermal management is essential.

Traditionally, air-cooling systems were used, but modern EVs now adopt liquid-cooling for better heat transfer. However, immersion cooling remains underutilized due to weight concerns. Our approach integrates Hybrid Single-Phase Cooling, combining air cooling from vehicle motion with immersion cooling. Immersion cooling offers uniform temperature regulation by addressing local heating on electrodes more effectively than indirect liquid cooling.

We propose three cases: a baseline with traditional cold plates, full immersion cooling with dielectric fluids, and comparisons between static and pumped immersion cooling. Key variables like fluid thermal conductivity and viscosity will be studied, alongside radial and axial cooling scenarios. Additionally, we will investigate battery pack arrangements, inspired by crystalline solid structures, to reduce weight and enhance heat transfer.

Using ANSYS Icepak, we will conduct CFD simulations on Lucid Motors' batteries, exploring cell orientations, geometries, and flow patterns to optimize cooling. This research aims to revolutionize EV thermal management, enabling high-power batteries to meet next-generation performance demands while improving energy efficiency and sustainability.

Keywords

Heat Transfer, Single-Phase Immersion Cooling, Direct-Liquid Cooling (DLC), Immersion Cooling, CFD Simulation, ANSYS Icepak, EV Batteries

Nomenclature

$\boldsymbol{q = Heat\ Generation\ (W)}$

$\boldsymbol{\Delta T = Temperature\ difference\ between\ batteries\ \&\ cooling\ fluid\ (K)}$

$\boldsymbol{\Delta P = Pressure\ drop\ between\ inlet\ \&\ outlet\ pressure\ (Pa)}$

$\boldsymbol{CFD = Computational\ Fluid\ Dynamics}$

$\boldsymbol{EV = Electric\ Vehicle}$

$\boldsymbol{ICE = Internal\ Combustion\ Engine}$

$\boldsymbol{BTMS = Battery\ Thermal\ Management\ System}$

$\boldsymbol{LIB = Lithium\ Ion\ Batteries}$

Introduction

The transportation industry is experiencing a significant shift as electric vehicles (EVs) increasingly replace internal combustion engine (ICE) vehicles, especially for personal transportation. This transition is driven by environmental concerns as a single ICE vehicle emits around 4.6 million metric tonnes of CO_2 in its every year, advancements in battery technology, improved motor efficiency, and the appeal of features like autonomous driving.

Like the heart of an ICE vehicle is an Internal Combustion Engine, in the same way, the heart of an EV is a DC Motor, which is powered by its battery pack. It directly influences charging time, range, cost, acceleration, and safety. Lithium-ion batteries are the preferred choice due to their high energy density, reliability, cost-effectiveness, and longevity. However, they are sensitive to temperature variations; operating outside the optimal range can degrade performance, shorten lifespan, or even lead to safety hazards like thermal runaway.

Maintaining safe battery temperatures under various conditions—such as sub-zero climates or rapid acceleration in hot environments—is crucial. To address this, Battery Thermal Management Systems (BTMS) have become essential in EV design. These systems monitor and regulate battery temperature through cooling mechanisms, performance throttling, or shutdowns to enhance reliability, efficiency, and safety. As batteries evolve to support faster charging and discharging, the demand for advanced thermal control solutions intensifies.

Recent advancements include the development of ultrafast charging technologies capable of charging batteries from 10% to 80% in under 11 minutes, addressing consumer concerns over long charging times. Additionally, innovations in battery swapping services are emerging as alternatives to traditional charging methods, aiming to reduce downtime and improve convenience for EV users.

Effective thermal management not only ensures safety but also prolongs battery life and optimizes performance, making it a critical focus in the ongoing evolution of electric vehicles.

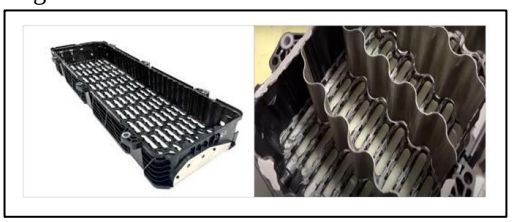

Figure 1: Lucid Motors Battery Pack

Lucid Motors is one of the biggest luxury EV makers in the world, with a market capitalization of $7.72 B and is currently growing at a breakneck pace. It is a technology company which focuses on manufacturing sustainable mobility, innovation, and high-performance EVs. For our research work, we had taken Lucid Motor's 117 kWh 900 V lithium-ion shown in figure 1, which is used in their upcoming model, the 2025 Lucid Air Grand Touring for our CFD simulations.

Cooling Methods & Theory

Notable methods of cooling are Single-Phase and Two-Phase Cooling. In a Single-Phase Cooling System, the fluid does not undergo phase change In a Single-Phase Cooling System, the fluid does not boil or undergo a phase change during anytime of the cooling process, while in the Two- Phase Cooling, the fluid boils and can undergo a phase change. includes Convection, where the fluid flows from the hot end to the cool end. The flow can be natural or forced. The working principle of this cooling is convection heat transfer, and the flow is buoyancy-driven. Single-Phase Cooling using a gaseous medium like air is used in many normal ICE vehicles as a standard and has plenty of standardization of operating procedures available.

The next in line is Single-Phase Liquid Cooling using a cold plate and microchannels, also called Direct Liquid Cooling (DLC) is much more effective than the method of air cooling, and modifications in the flow patterns can lead to achieve even better performances in heat exchange. Cooling can also be achieved using the method of immersion cooling, wherein the battery is immersed into a dielectric fluid which is in circulation either by natural convection or by an external pump. This method can also be used as a Single-Phase Cooling, but it is mainly used as a Two-Phase Cooling method. This is one of the best technologies available for cooling of electronics. The liquid absorbs the heat from the device and then is passed through a heat exchanger to cool the fluid. The method of Two-Phase Cooling is an area of immense possibilities. Research with two-phase liquid cooling suggests a tremendous leap in higher heat transfer rates and improved thermal performance as the thermal resistance decreases drastically in the Two-Phase Flow, compared to Air Cooling or Single-Phase Liquid Cooling. However, designing and managing such systems is more complex due to the need to control the phase transition and ensure proper flow distribution. This complex flow and heat transfer phenomenon is challenging to solve for velocity fields numerically and validate using experimental setups. So, for our simulations, we focused on Single Phase Cooling in the form of Immersion Cooling. This can be seen in our simulations, as well, where we have simulated the EV Battery cooling using only Single-Phase Cooling using a draft of air on the battery pack, as the average chip temperatures reached a staggering 230 °C (503.15 K) at a normal discharge rate of 1 C. Then we did a cold plate based direct liquid cooling simulation for our battery and got a reasonable temperature of 31.02 °C (304.17 K) at 1C discharge rate, but as we went on increasing the power rate at higher discharge rates, the maximum temperature of the cells was going above the suitable operating range. So, we believe that Single-Phase Liquid Cooling using Immersion Cooling is a much more effective method of cooling our EV batteries. We will talk about these different cooling methodologies in the BTMS section of the report.

Heat generation in Lithium-Ion Batteries (LIBs) is a result of multiple factors, primarily classified as ohmic (Joule) heating, reversible heat generation, and reaction heat generation. These can be expressed by the following equation:

$$Q_{total} = Q_{ohmic} + Q_{reaction} + Q_{reversible}$$

$$Q_{ohmic} = i^2 R$$

$$Q_{reversible} = iT\frac{dV_{oc}}{dT}$$

Ohmic heating is due to the internal resistance of the battery. Reversible heat generation occurs due to entropy changes during the electrochemical reactions within the battery, and reaction heat generation results from exothermic and endothermic reactions during charging and discharging. These types of heat generation contribute to temperature gradients within the battery cells, creating the need for efficient thermal management to prevent uneven heat distribution, which can accelerate degradation and pose safety risks. LIBs operate best in a narrow temperature range of 25-40°C to optimize performance and safety, and exceeding 60°C can lead to severe safety issues such as thermal runaway.

The heat transfer rate is higher when the flow's Reynolds number increases. The flow is considered Laminar at low Reynold's Number ($R_e < 2300$). In Single-Phase Immersion Cooling, convective heat

transfer is enhanced by turbulence created in the flow due to the problem being considered as a flow over a cylinder. Increasing the flow rate will increase the Reynolds number and the vehicle being in motion will have vibrations, which will cause the flow to become turbulent over the length of the battery pack, but we are limited by the pump power and the battery electronics are sensitive and high flow velocities will damage the electronics, so we cannot have very high velocities of the fluid flowing through the Battery.

Battery Thermal Management System

A Battery Thermal Management System (BTMS) is a combination of components and control algorithms dedicated to monitoring and maintaining the battery pack's temperature within its optimal range, whether through cooling or heating. As EV batteries experience dynamic operating conditions, the BTMS must adapt to varying thermal loads and environmental factors to ensure the battery functions efficiently and safely.

Temperature has a profound impact on battery performance and longevity. At low temperatures, the battery's internal resistance increases, significantly reducing power output and charge acceptance. For instance, studies have shown that lowering the battery temperature from 25°C to -15°C can result in a state-of-charge loss of approximately 23%. On the other hand, elevated temperatures can accelerate battery degradation and pose a risk of thermal runaway, a dangerous condition where excessive heat leads to a self-sustaining reaction, potentially causing fire or explosion. An effective BTMS actively regulates the thermal environment of the battery pack, mitigating these risks. By maintaining the battery within a safe operating temperature range, BTMS improves energy efficiency, reliability, and safety while extending the battery's operational lifespan. Modern BTMS designs include advanced cooling technologies such as liquid cooling, immersion cooling, and integrated phase-change materials, tailored to manage the heat generated during fast charging, rapid acceleration, or high ambient temperatures.

Furthermore, with the rise of next-generation EV batteries capable of ultra-fast charging (e.g., reaching 80% in under 10 minutes), the demands on thermal management systems are increasing. Advanced BTMS solutions are incorporating machine learning and predictive algorithms to dynamically adjust thermal responses based on usage patterns, environmental conditions, and battery health. These innovations not only ensure safety but also enable the development of more compact and lightweight battery systems, contributing to greater energy efficiency and overall vehicle performance.

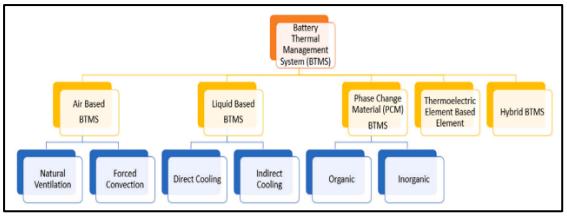

Figure 2: Classification of BTMS

While there are multiple cooling technologies available for electric vehicle (EV) batteries, two Battery Thermal Management System (BTMS) solutions dominate the commercial space today:

Air Cooling: Air cooling is the simplest, most lightweight, and cost-effective option. It relies on either natural or forced airflow to dissipate heat from the battery pack. However, it has significant limitations due to air's relatively low thermal conductivity and specific heat capacity, making it unsuitable for high-power EVs. Air cooling struggles to manage the thermal loads generated during fast charging or rapid acceleration, leading to inefficiencies in temperature regulation and potential battery degradation over time.

Indirect-Liquid Cooling: Cold-plate cooling, also known as indirect liquid cooling, is a step up in complexity and efficiency compared to air cooling. In this method, a coolant liquid—typically a water-glycol mixture—circulates through metal plates with embedded channels that are in physical contact with the battery cells. This approach leverages the high thermal conductivity of metals and the superior specific heat capacity of the liquid coolant to remove heat more effectively. However, a common challenge with cold-plate cooling is the formation of hot spots within the battery. These localized high-temperature regions accelerate battery aging, reduce overall capacity, and may even act as triggers for thermal runaway if not addressed properly.

Immersion Cooling: Immersion cooling, also known as direct liquid cooling, is an advanced cooling method that combines the benefits of both air and indirect liquid cooling. In this technique, the battery cells are entirely submerged in a dielectric fluid with a high specific heat capacity. This enables a more uniform temperature distribution across the cells, significantly reducing hot spots and improving overall thermal management. Immersion cooling also enhances the battery's safety and lifespan. However, it is not widely adopted in commercial EVs today due to the added weight and cost associated with dielectric fluids and system design. Despite these challenges, immersion cooling has immense potential, particularly for next-generation EVs with higher power requirements.

Design Modelling

Currently, most companies, such as Tesla, Lucid Motors, BMW (for i8 and i3), etc., are using indirect liquid cooling technologies. Indirect liquid cooling mainly involves coolant flowing through pipes or

cold plates and similar devices. Lucid Motors uses Li-ion batteries made by LG Chem. There are 300 cells in each Lucid module. Hence, the 22 module models contain 6,600 individual cylindrical cells. Each module comprises an injection-molded plastic case that includes ten groups of 300 cells separated by thermos-formed mica sheets. The cells are free-floating in the modules and, unlike other packs, do not have a potting system to hold the individual cells in place. The batteries get heated more axially than radially; hence, Lucid motors use a cooling plate for their modules, which cools from the axial end of the battery cylinder.

We were initially focused on simulating the cooling of the entire battery pack of 6600 cells, but unfortunately due to lack of time and lack of resources, we had to cut down to simulating 9 cells. The geometry of the cells is attached in figure 3.

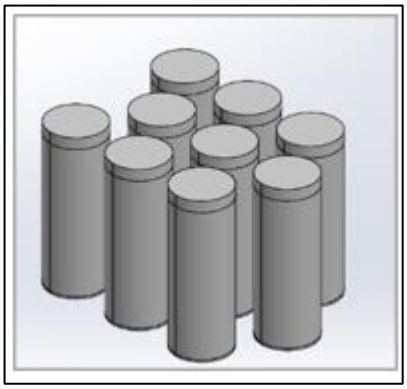

Figure 3. 3x3 Battery CAD (Simplified)

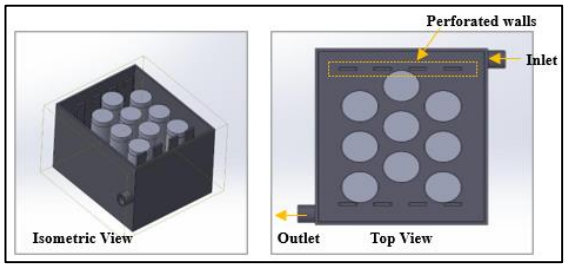

Figure 4. Different views of Battery CAD

Through our project, we want to simulate two different types of immersion cooling (forced and static) to cool the entire battery module directly, and with this, we expect the benefits of reduction in the hot spots, uniform cooling across all cells reducing thermal fluctuations and better thermal management compared to cold plates. We will be comparing this results with the current available cooling methodologies of air cooling and cold-plate based indirect liquid cooling.

We used cells from model 21700 in our design and a battery module of 3x3 battery cells (9 cells arranged in a honeycomb structure). Figure 4 shows the design of the Direct Liquid Cooling System our team developed for the batteries. It has an inlet, outlet, and perforated walls through which the dielectric fluid flows. The cold plate used by the lucid motors is a two-piece aluminum stamping. It has dimples bonded to hold two pieces of aluminum to resist the pressure of water-glycol pumped in and out from the unions (inlet and outlet, as shown in figure 5 & 6). The dimples also induce turbulent flow to the fluid for better heat removal.

Figure 5. Lucid Motors Cold Plate design

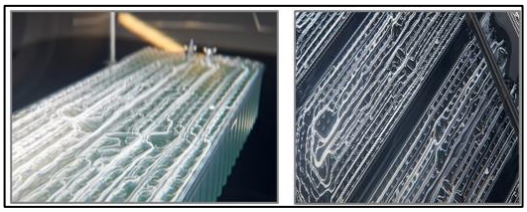

Figure 6. Coolant flowing through channels of cold plate and cooling the batteries

We divided the battery cell into four components: the anode, cathode, central graphite rod, and jelly roll material. The anode and cathode are made of aluminum, the central graphite rod is made of graphite, and the jelly roll is a custom material, whose properties are given below. The cell is attached in figure 7. The thermal conductivity of Jelly Roll (place where the heat is being generated), is anisotropic in nature, and its thermal conductivity has 3 components (z,θ,r).

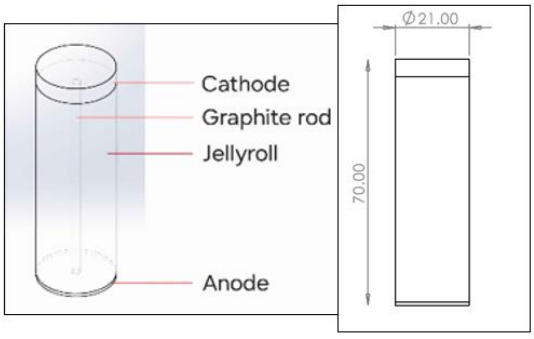

Figure 7. Internal Structure of cell & its dimensions

Parameter	Value
Graphite Thermal Conductivity (W/mK)	50
Graphite Density (kg/m^3)	1800
Graphite Specific heat (J/kgK)	940
Aluminium 1100 Thermal Conductivity (W/mK)	218
Aluminium 1100 Density (kg/m^3)	2710

Aluminium 1100 Specific heat (J/kgK)	900

Jellyroll	Value
Thermal Conductivity (z) (W/mK)	0.29
Thermal Conductivity (θ) (W/mK)	25
Thermal Conductivity (r) (W/mK)	32.2
Density (kg/m^3)	2560
Specific Heat (J/kgK)	1000

The dimensions of each component of the cell are as follows:

- Anode - 1mm x 21mm
- Jelly roll - 61mm x 21mm
- Cathode - 5mm x 21mm
- Graphite rod - 64mm x 2.3mm

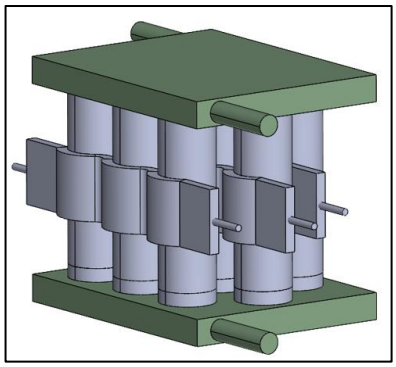

Figure 8. Cold Plate Design

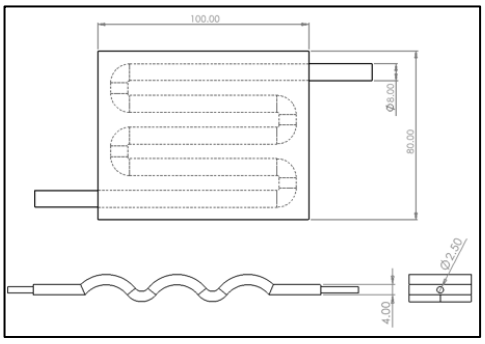

Figure 9. Cold Plate Dimensions

The cold plate is made of extruded aluminium material. Its properties are given in the table below.

Parameter	Value
Thermal Conductivity (W/mK)	205
Density (kg/m^3)	2800
Specific heat (J/kgK)	900

The cold plate was designed in such a way so as to keep the temperatures minimum at the longitudinal and the axial areas, as the thermal conductivities are different due to the anisotropic nature, we can see that the heat dissipation rate is different in these 2 directions. Exact design of the cold plate was not available on the internet due to proprietary issues, so we made our cold plate as much similar to normal available cold plates as possible.

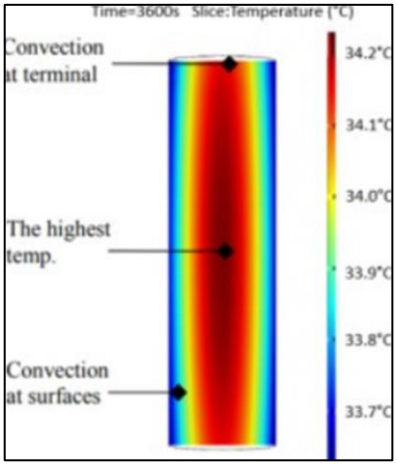

Figure 10. Heat Dissipation difference in different directions.

The total surface area of the cells is 5309.86 mm^2. For our design of forced immersion cooling, we also tried 6 different dielectric fluids. The fluids used were Mineral oil, Silicone 100, Toulene, NOVEC 7500, NOVEC 7200 and Ethylene Glycol 50-50.

Mineral Oil	Value
Thermal Conductivity (W/mK)	0.13
Density (kg/m^3)	849.3
Specific Heat (J/kgK)	1680
Thermal Expansion Coefficient (K^{-1})	0.00064
Molecular Mass (kg/mol)	0.40561
Dynamic Viscosity (kg/ms)	0.0194

Silicone 100	Value
Thermal Conductivity (W/mK)	0.1
Density (kg/m^3)	890
Specific Heat (J/kgK)	1673.6
Thermal Expansion Coefficient (K^{-1})	0.00097
Molecular Mass (kg/mol)	0.074
Dynamic Viscosity (kg/ms)	0.003

Toulene	Value
Thermal Conductivity (W/mK)	0.134
Density (kg/m^3)	862
Specific Heat (J/kgK)	1260
Thermal Expansion Coefficient (K^{-1})	0.00108

Molecular Mass (kg/mol)	0.0921
Dynamic Viscosity (kg/ms)	0.00056

NOVEC 7500	**Value**
Thermal Conductivity (W/mK)	0.065
Density (kg/m^3)	1614
Specific Heat (J/kgK)	110
Thermal Expansion Coefficient (K^{-1})	0.00129
Molecular Mass (kg/mol)	0.414
Dynamic Viscosity (kg/ms)	0.000807

Ethylene Glycol 50-50	**Value**
Thermal Conductivity (W/mK)	0.41
Density (kg/m^3)	1060
Specific Heat (J/kgK)	3504
Thermal Expansion Coefficient (K^{-1})	0.00057
Molecular Mass (kg/mol)	0.0621
Dynamic Viscosity (kg/ms)	0.0028

NOVEC 7200	**Value**
Thermal Conductivity (W/mK)	0.069
Density (kg/m^3)	1430
Specific Heat (J/kgK)	1213.36
Thermal Expansion Coefficient (K^{-1})	0.0016
Molecular Mass (kg/mol)	0.264
Dynamic Viscosity (kg/ms)	0.00061

Then once we have these fluids, we went ahead and simulated our design for a discharge rate of 2 C 4 lpm for the 6 fluids to get a comparison of the dielectric liquids. Then from them, we selected Mineral Oil due to the best material compatibility with the batteries for our future CFD simulations.

Computational Fluid Dynamics (ANSYS Icepak)

Computational Fluid Dynamics (CFD) enables the modeling of fluid mechanics and heat transfer principles to optimize thermal management systems. Key aspects include laminar flow, Navier-Stokes equations, volumetric heat generation, and temperature gradients. CFD uses techniques like Finite Volume, Finite Element, and Finite Difference methods, with Finite Volume being most common. The process involves meshing the model geometry into segments, solving governing equations iteratively until convergence is reached, providing insights into flow velocity, turbulence, temperature, and energy balance.

ANSYS Icepak, a Finite Volume-based solver, is used for our study to analyze thermal properties and fluid dynamics for immersion and hybrid cooling. Icepak includes all modes of heat transfer (conduction, convection, radiation) for steady-state and transient applications. Its Sparse Direct Solver optimizes simulations by minimizing operation counts, making it dynamic and efficient.

The Icepak process begins with importing the geometric CAD model, defining boundaries, and applying cooling components like heat sinks and cold plates. Material properties, such as lithium cells and aluminum casing, and fluid properties, including cooling solutions, are assigned. Constraints like flow rates, fan speeds, and heat loads are applied. The model is then meshed, and simulations run iteratively to solve governing equations. Results are presented numerically or visually, enabling evaluation of cooling performance.

The governing equations are given as follows:

1. $\nabla . \overrightarrow{u_c} = 0$ (continuity equation for the coolant)
2. $\rho_c \frac{\partial \overrightarrow{u_c}}{\partial t} + (\overrightarrow{u_c} . \nabla)\overrightarrow{u_c} = -\nabla p + \mu_c \nabla^2 \overrightarrow{u_c} + \rho_c g$ (Navier Stokes Equation for the coolant)
3. $\frac{\partial T_c}{\partial t} + (\overrightarrow{u_c} . \nabla)T = \frac{K_c}{\rho_c C_{p_c}} \nabla^2 T_c$ (Heat Conduction Equation for the coolant)
4. $\frac{\partial T_{cell}}{\partial t} = \frac{K_{cell}}{\rho_{cell} C_{p_{cell}}} \nabla^2 T_{cell} + q_{cell}$ (Heat Conduction Equation for the battery cell)
5. $q_{cell} = i^2 R$ (Heat Generation insdie the battery cell)
6. $\frac{\partial T_{cp/imm}}{\partial t} = \frac{K_{cp/imm}}{\rho_{cp/imm} C_{p_{cp/imm}}} \nabla^2 T_{cp/imm}$ (Heat Conduction Equation for Cold Plate/ Immersion Cooling Enclosure)
7. $\frac{\partial \rho_a}{\partial t} + \nabla . (\rho_a \overrightarrow{u_a}) = 0$ (continuity equation for air)
8. $\frac{\partial (\rho_a \overrightarrow{u_a})}{\partial t} = -\nabla p + \mu_a [\nabla^2 \overrightarrow{u_a} + \frac{1}{3} \nabla (\nabla . \overrightarrow{u_a})] + \rho_a g$ (Navier Stokes Equation for air)
9. $\frac{\partial (\rho_a T_a)}{\partial t} = \frac{K_a}{C_{p_a}} \nabla^2 T_a$ (Heat Conduction Equation for air)
10. $\rho_a = \frac{p_a}{R T_a}$ (Ideal gas law)

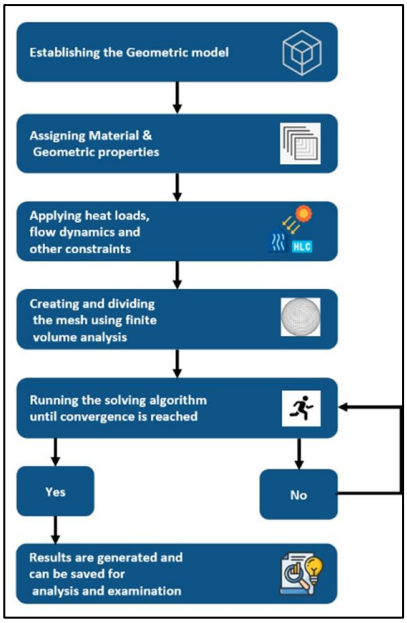

Figure 11.Working of ANSYS Icepak.

Methodology & Boundary Conditions

The model does not consider thermal resistance of the thermal paste and contact resistance between the components, and we had assumed the ideal condition of 0 thermal contact resistance. With focus on relative gains in cooling for different flow rates and discharge rates.

The generated SolidWorks designs were imported to the ANSYS AEDT in the form of .STP or a .IGES file. We went ahead with the following boundary conditions:

Parameter	Value
Discharge Rates	0.5 C, 1.0 C, 1.5 C, 2.0 C, 2.5 C, 3.0 C
Volumetric Flow Rate (lpm)	2, 4, 6
Fluid Inlet Temperature	25 °C (298.15 K)

The simulation was carried out with the following conditions, the solver was set to Pressure based, because we considered the fluid to be liquid, which is considered as incompressible. We set the solution to be a steady state solution and the number of iterations were set as 500. The viscous model was set as Enhanced Realizable Two Equation for turbulence modelling. The scheme was set to coupled velocity pressure formulation and the flow and energy equations were solved sequentially. The heat value was assigned to the jelly roll as all the chemical reactions occur over there in a cell, and it was assigned as a block. The walls were set at ambient temperature and as stationary, and only for the flow immersion and forced air cooling, the inlet and outlet was set. It was set in such a way that the pressure for the outlet was set to ambient, so as to get the gage pressure value during computation of the pressure drop.

We set the offset padding as 10 to get the enclosure in all direction for static cooling and as 15 in the flow direction, wherever we had a flow.

The convergence criterion was set as follows:

Parameter	Convergence Value
Continuity	1e-12
X - Velocity	1e-12
Y – Velocity	1e-12
Z – Velocity	1e-12
Energy	1e-12

ANSYS Icepak was not allowing us to simulate the battery's discharge rate, and so we have to model it as a constant heat source for a particular discharge rate. The internal resistance of the 21700 battery is 12 mΩ, and the battery capacity of this battery is 4000 mAh. Then we used the following formulas to get the values of heat corresponding to the discharge rates (These values are for 1 cell):

$$I = Battery\ Capacity * C - rate$$

$$Q = I^2R$$

Discharge Rate (C)	Current (A)	1 cell Q (W)	Total Q (W)
0.5	2	0.048	0.432
1.0	4	0.192	1.728
1.5	6	0.432	3.888
2.0	8	0.768	6.912
2.5	10	1.2	10.8
3.0	12	1.728	15.552

With these above-mentioned boundary conditions. We ran our simulations for 5 main cases, which are the forced air cooling, the static air cooling, the forced immersion cooling, the static immersion cooling and the cold plate based cooling (Baseline data). We ran all our simulations, a total of 90 simulations and then from there, we were able to figure out if our hypothesis of single phase immersion cooling is better or no as compared to other cooling methodologies available. All the above boundary conditions were either taken from ANSYS or from the literature.

Grid Independence

Along with our initial simulations we also performed a mesh independence study. Mesh independence is when the simulation results are not affected by the quality of the mesh during element analysis. It is important to determine because if the mesh setting is affecting the final result of each simulation, then we would need to reconstruct our solution method. If we see consistent results

between settings then we know the solution is independent from the mesh.

To determine mesh independence, we looked at two different values: Pressure drop, and temperature. Using a flow immersion simulation model with a discharge rate of 2C and 2 lpm, the main change done was to the mesh quality. Icepak has five general mesh settings, which were applied to the model before running the simulation. The number of elements for each setting is listed below in the table along with their element size in mm. The values for minimum and maximum temperature were recorded after each simulation along with pressure drop. These graphs help us conclude that the simulation results for our batteries becomes independent around an element size of 0.033 mm in all directions. That is the size used by the third setting and afterwards temperature becomes linear for the remaining two. Pressure drop levels out around the fourth setting, but it remains independent afterwards. At the finest setting for our simulations, the number of elements was counted to be around 679,568 with an element size of 0.025 mm. Visually, there are also indications of how the mesh becomes more uniform the higher the quality.

Another thing to note is the convergence of each simulation. The time it took to run all five simulations varied significantly based on the number of elements in the mesh. The coarse setting only took two minutes at most while the fine setting took at minimum thirty minutes to an hour. There is a clear indication of how convergence applies to the mesh setting since it has more elements to analyze, but the end results give us better quality values for temperature, velocity and pressure drop for immersion cooling.

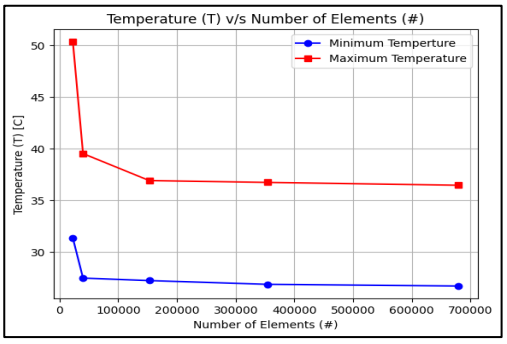

Figure 12. Temperature v/s # Elements.

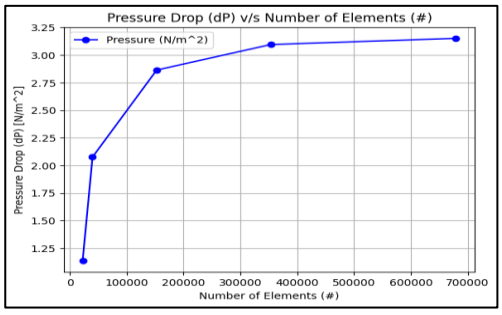

Figure 13.Pressure Drop v/s # Elements.

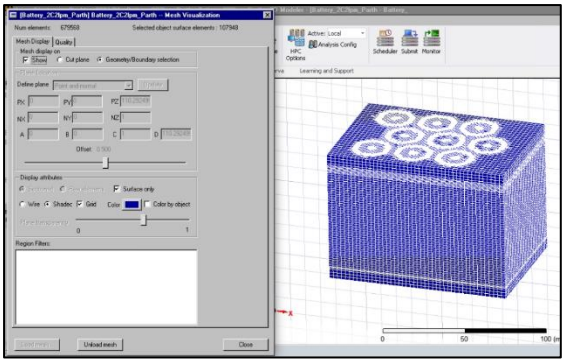

Figure 14. Mesh.

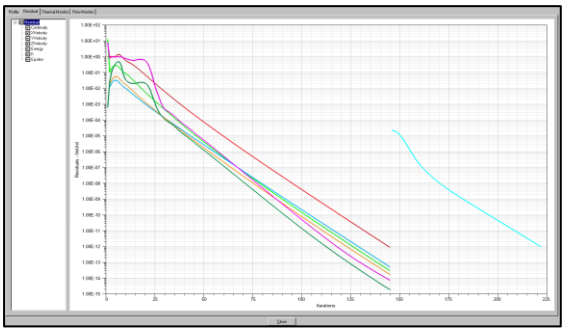

Figure 15. Convergence Plot.

Mesh Level	# Elements	Element Size
1	22523	0.05
2	39898	0.045
3	152817	0.033
4	353570	0.03
5	679568	0.025

Different Fluid Study

We studied the 6 different fluids, the results are attached for them below. We ran 6 simulations for 2 C discharge rate and 4 lpm flow rate.

The analysis of the maximum temperature (T_{max}) and temperature difference (ΔT) highlights the superior cooling performance of EG 50/50. It achieves the lowest T_{max} of approximately 25 °C, while other fluids, such as toluene, Novec 7200, Novec 7500, and Silicone 100, exhibit T_{max} values around 30 °C. This lower Tmax indicates better heat dissipation capabilities for EG 50/50. The temperature difference (ΔT) further supports this, as EG 50/50 exhibits the smallest ΔT (~1 °C), reflecting minimal thermal resistance. On the other hand, fluids like mineral oil show a higher T_{max} and a lower ΔT (~0.5 °C), suggesting it maintains thermal stability but lacks the cooling efficiency seen with EG 50/50 and Novec fluids. Novec 7200 and Novec 7500 also demonstrate competitive thermal performance, with consistent T_{max} values and small temperature differences, making them viable alternatives for applications requiring effective cooling. When evaluating pressure drop (ΔP) and overall system efficiency, EG 50/50 stands out with its high figure of merit (~80), reflecting excellent thermal performance and manageable

hydraulic behavior. Mineral oil shows a significant pressure drop (~6 N/m²), which can pose challenges in pumping requirements, despite its stable thermal behavior. Toluene, Novec 7200, and Novec 7500 exhibit lower pressure drops (<1 N/m²), making them more energy-efficient for fluid circulation in cooling systems. However, their figure of merit remains lower compared to EG 50/50. Silicone 100 and mineral oil, while showing decent figures of merit (~40), lag behind EG 50/50 and the Novec fluids due to their higher pressure drops and less efficient cooling capabilities. Overall, EG 50/50 proves to be the most efficient cooling fluid, balancing excellent thermal performance with favorable hydraulic properties.

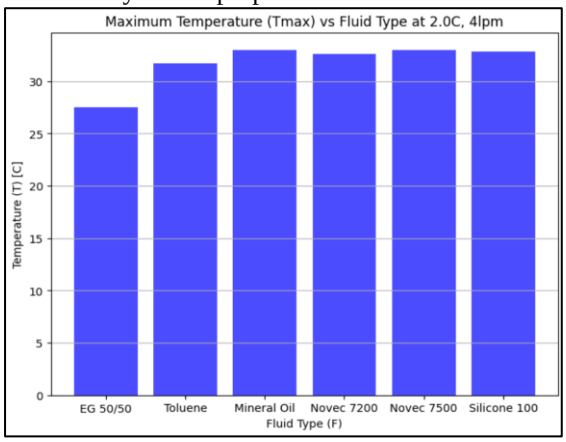

Figure 16. Cell Maximum Temperature v/s Fluid Type.

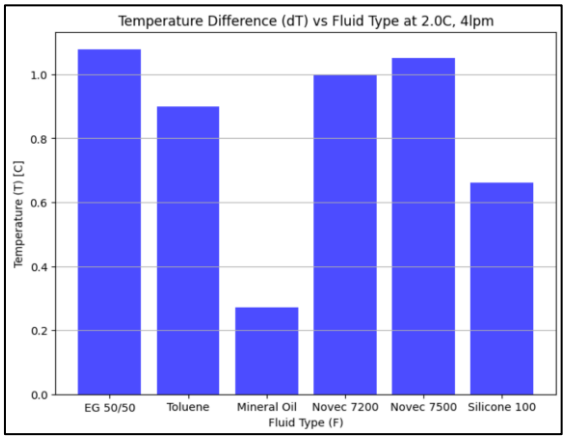

Figure 17. Fluid Temperature Rise v/s Fluid Type.

The figure of merit (FOM) is a critical metric that evaluates the suitability of fluids for convective immersion cooling applications, combining their thermal and hydrodynamic properties. In this study, six fluids were assessed under identical conditions: mineral oil, silicone 100, toluene, NOVEC 7500, ethylene glycol (50-50), and NOVEC 7200. Ethylene glycol (50-50) demonstrated the highest FOM of 85.46, correlating with its lowest maximum cell temperature of 27.488°C at a 2C discharge rate and 4 LPM flow. This highlights its superior thermal conductivity and heat transfer efficiency, making it the most effective fluid for reducing thermal hotspots under convective immersion cooling. Among the other fluids, mineral oil, silicone 100, and toluene exhibited FOM values of 28.890, 24.60, and 26.91, with corresponding maximum cell temperatures of 33.007°C, 32.802°C, and 31.745°C, respectively. These results suggest that toluene, despite its moderate FOM, performed slightly better in maintaining lower cell temperatures than silicone 100 and mineral oil, underscoring its thermal efficiency in the given flow conditions.

For the NOVEC fluids, NOVEC 7500 and NOVEC 7200 recorded FOM values of 18.80 and 20.21, respectively, with maximum cell temperatures of 32.973°C and 32.613°C. While their maximum temperatures were comparable to those of mineral oil and silicone 100, their lower FOM values indicate a trade-off in thermal conductivity or convective efficiency. These findings reinforce the importance of correlating FOM with real-world thermal performance, as fluids like ethylene glycol (50-50) clearly outperform others in both metrics. For applications requiring the highest thermal management efficiency, ethylene glycol is the most favorable choice, while the other fluids may be considered for less demanding cooling scenarios where other factors such as environmental impact or chemical stability play a more significant role.

$$FOM = k\left[\frac{\rho Cp}{k}\right]^{1/3}$$

where:

ρ = Density, kg/m3

k = Thermal conductivity, W/mK

Cp = Specific Heat, J/kg

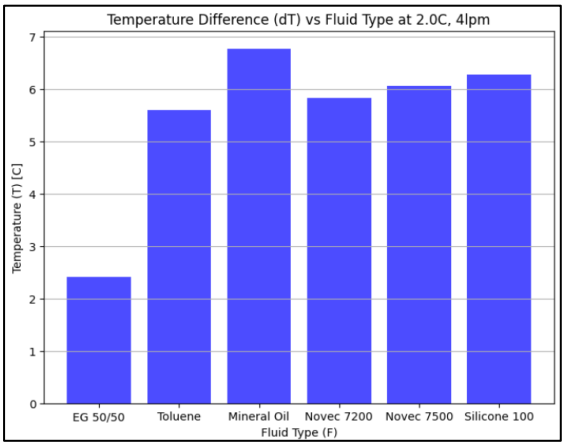

Figure 18. Delta T of Cells v/s Fluid Type.

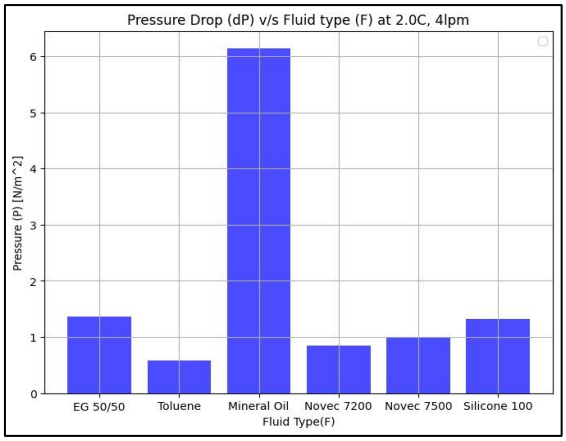

Figure 19. Pressure Drop v/s Fluid Type.

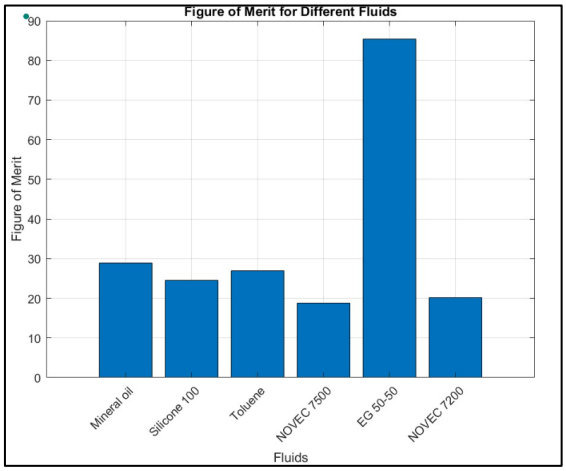

Figure 20. Figure of Merit Plot.

Global Warming potential

The selection of coolants for EV battery thermal management systems must account for their Global Warming Potential (GWP), flammability, and toxicity, as these factors influence the overall environmental impact, safety, and regulatory compliance of electric vehicles. Balancing thermal performance with sustainability is essential to align EV technology with environmental goals.

Global Warming Potential measures a substance's capacity to trap heat in the atmosphere compared to CO_2 (GWP = 1). Coolants with high GWP significantly contribute to climate change, offsetting the environmental benefits of EVs.

Low-GWP Coolants:

Silicone 100 (GWP 2.5) and Toluene (GWP 1.47) are excellent choices for reducing greenhouse gas emissions while maintaining effective heat transfer properties.

Novec 7200 (GWP 55) and Novec 7500 (GWP 90), though higher, remain far below traditional refrigerants like HFCs (with GWPs in the thousands).

Significance:

Using low-GWP coolants helps meet global climate regulations such as the Kigali Amendment and regional policies like the EU F-Gas Regulation.

This ensures the thermal management system's sustainability over its life cycle, minimizing environmental impact.

Flammability:

Flammability is a critical safety concern in EVs, particularly during thermal runaway events or accidents. The risk of coolant ignition can compromise battery safety and lead to severe environmental damage if fires release toxic fumes.

Non-Flammable Options:

Novec 7500, Novec 7200, and Silicone 100 are non-flammable, ensuring safe operation under extreme thermal conditions.

These coolants are preferred for safety-focused designs and applications where flammability must be minimized.

High-Flammability Risks:

While toluene offers excellent heat transfer and low GWP, it is highly flammable and requires stringent safety measures, such as secure containment systems and fire prevention protocols.

Flammable coolants can pose risks during leaks or high-heat scenarios, necessitating additional safety infrastructure.

Toxicity:

Toxicity determines a coolant's impact on human health and the environment during leaks, spills, or disposal. Toxic coolants can contaminate soil and water sources, posing long-term environmental risks.

Environmentally Safe Options:

Silicone 100, Novec 7500, and Novec 7200 are low-toxicity and non-hazardous, making them safe for handling and less impactful during accidental leaks.

These coolants also simplify end-of-life disposal, reducing environmental remediation efforts.

High-Toxicity Coolants:

Ethylene Glycol, widely used in cooling systems, is toxic if ingested and can contaminate water sources, requiring robust containment and disposal strategies.

Toluene is volatile and toxic, posing risks to human health and ecosystems if not managed carefully.

Combined Environmental Impact:

The overall environmental impact of a coolant is determined by its balance between GWP, flammability, and toxicity. The table below summarizes these aspects:

Coolant	GWP	Flammability	Toxicity	Key Notes
Silicone 100	2.5	Non-flammable	Very low	Environmentally safe, highly stable.

Novec 7500	90	Non-flammable	Low	Good thermal performance, low GWP.
Novec 7200	55	Non-flammable	Low	Moderate GWP, efficient cooling.
Ethylene Glycol	-	Moderate	High	Toxic; widely used but environmentally risky.
Toluene	1.47	Highly flammable	High	Excellent heat transfer but risky.

Key Considerations for Coolant Selection:

When selecting coolants for EV battery thermal management systems, balancing performance and environmental impact is crucial:

- Low-GWP coolants like Silicone 100 and Toluene minimize climate change contributions but must address safety concerns.
- Non-flammable options such as Novec 7500, Novec 7200, and Silicone 100 ensure operational safety while reducing environmental risks.
- Low-toxicity coolants are essential to avoid contamination and simplify disposal, making Silicone 100 and Novec coolants the most favorable options.

By integrating low-GWP, non-flammable, and non-toxic coolants, EV battery systems can reduce their environmental footprint while enhancing safety and regulatory compliance. Careful selection of coolants ensures that the EV industry continues to lead in sustainability and environmental responsibility.

Ground Truth Simulation

Now, we simulate the mineral oil fluid for all the 6 discharge rates and 3 flow rates and get the results for the cold plate, which is our ground truth data, to which we want to compare the results. The table is only for data of 3 discharge rates at 2, 4, 6 lpm respectively.

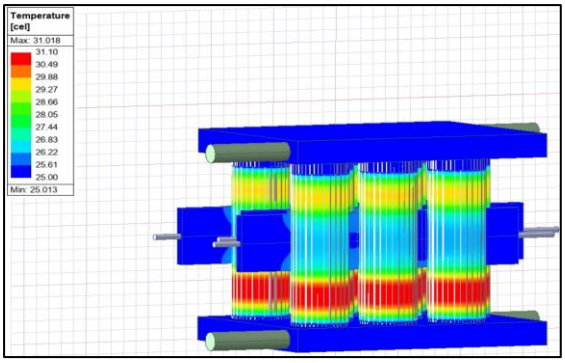

Figure 21. 1 C Discharge Rate 4 lpm.

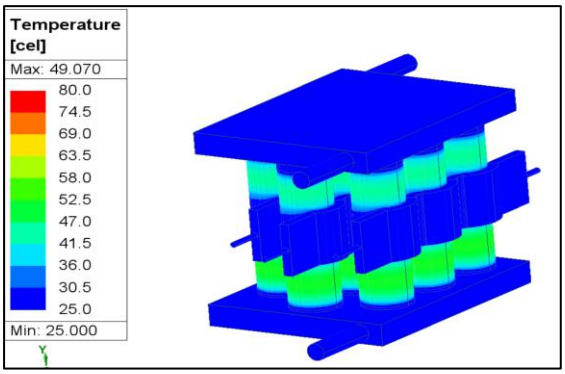

Figure 22. 2 C Discharge Rate 4 lpm.

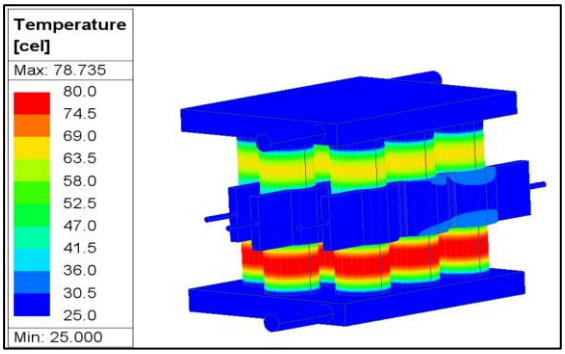

Figure 23. 3 C Discharge Rate 4 lpm.

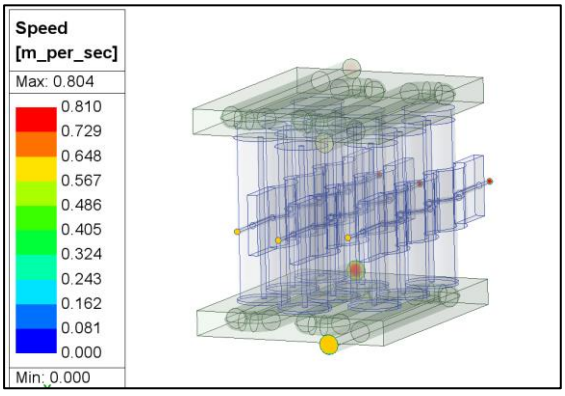

Figure 24. Speed Plot for 4 lpm.

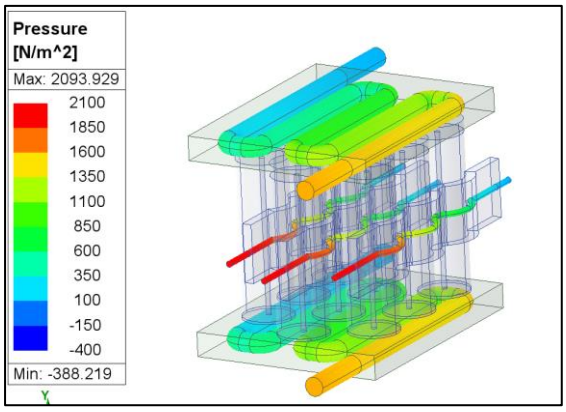

Figure 25. Pressure Drop plot for 4 lpm.

Discharge Rate (C)	Max Temperature (°C)	Del P (N/m^2)	Del T (°C)
1	31.168	757.325	6.143
2	49.671		24.671
3	90.518		65.518
Discharge Rate (C)	Max Temperature (°C)	Del P (N/m^2)	Del T (°C)
1	31.018	2236.875	6.005
2	49.07		24.07
3	78.735		53.735
Discharge Rate (C)	Max Temperature (°C)	Del P (N/m^2)	Del T (°C)
1	30.949	4285.833	5.941
2	48.797		23.797
3	78.135		53.135

Main Simulation Results

Here, we have 4 different cases for simulation (Static Air, forced Air, Static Immersion and Forced Immersion). we simulate the mineral oil fluid for all the 6 discharge rates and 3 flow rates and get the results for the above cases. We did the forced air for only 1 case, 1 C 4 lpm, and the temperatures were very unreasonable and so we left that case and focused on other cooling methodologies. For Static Air cooling and Static Immersion cooling, it acted as if it was a giant heat spreader.

Static Air Cooling: The table given is for 3 discharge rates, here, we do not have flow so, we don't have any velocity vectors. The velocity is almost negligible as there is no flow and the minimal velocity is due to the convection currents set up at the boundary due to heat generation.

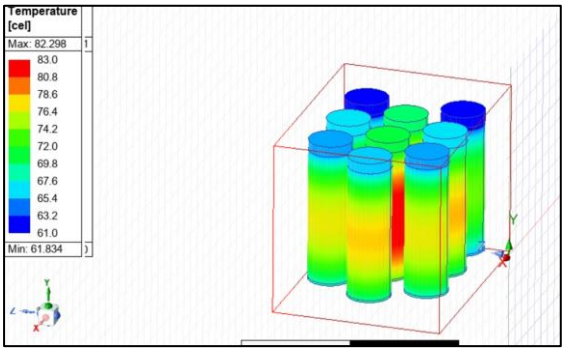

Figure 26. 1 C Discharge Rate.

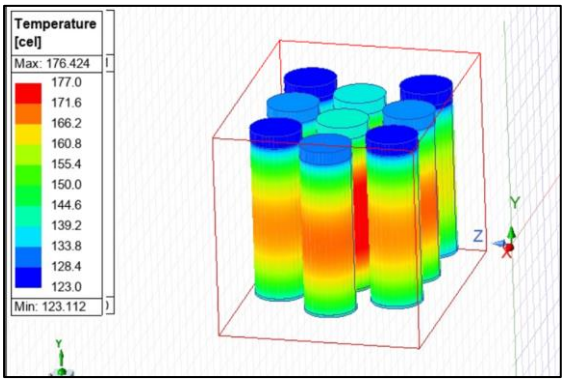

Figure 27. 2 C Discharge Rate.

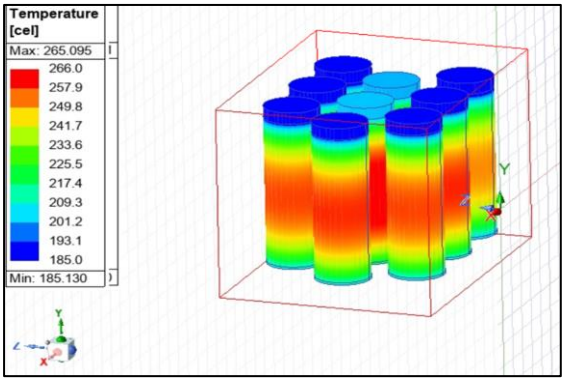

Figure 28. 3 C Discharge Rate.

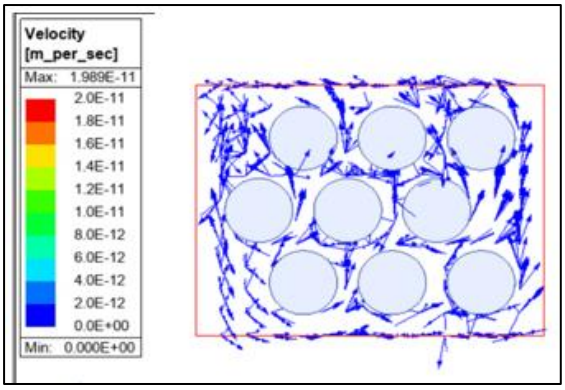

Figure 29. Velocity Vectors.

Discharge Rate (C)	Max Temperature (°C)	Del T (°C)

1	82.3	20.5
2	176.4	53.3
3	265	79.9

Static Immersion Cooling: The table given is for 3 discharge rates, here, we do not have flow so, we don't have any velocity vectors. The velocity is almost negligible as there is no flow and the minimal velocity is due to the convection currents set up at the boundary due to heat generation.

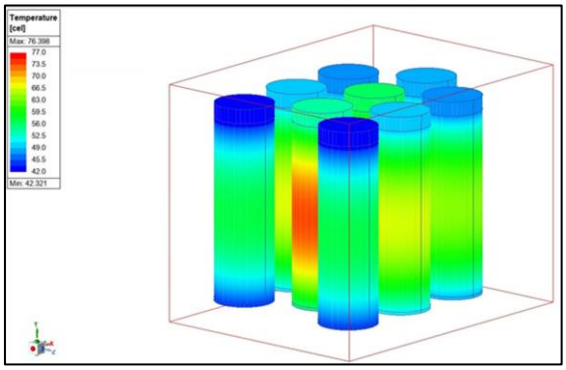

Figure 30. 1 C Discharge Rate.

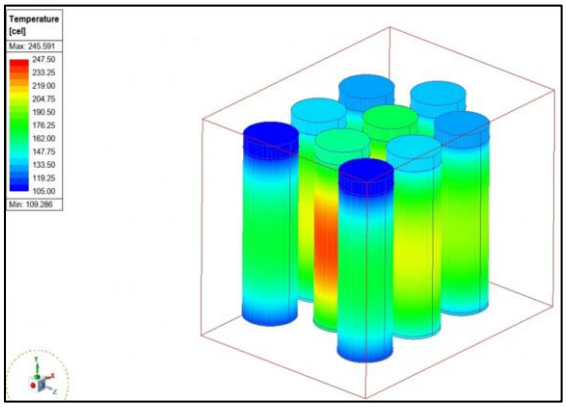

Figure 31. 2 C Discharge Rate.

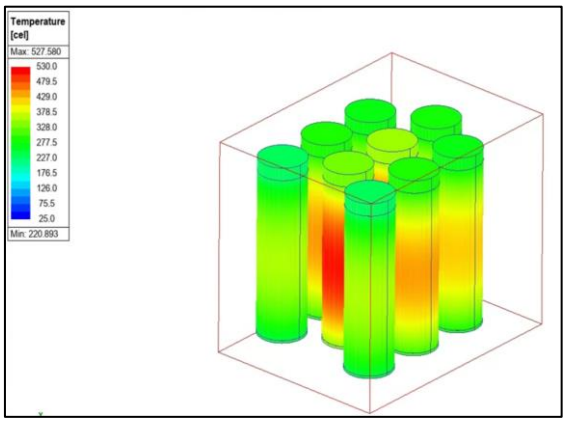

Figure 32. 3 C Discharge Rate.

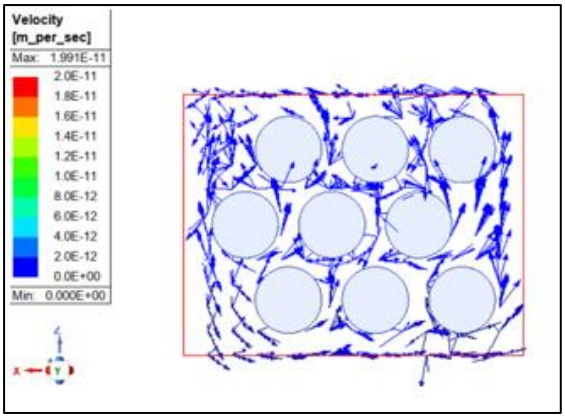

Figure 33. Velocity Vectors.

Discharge Rate (C)	Max Temperature (°C)	Del T (°C)
1	76.4	34.1
2	245.6	136.3
3	527.6	306.7

Forced Air Cooling: We did just one simulation with 1 C 4 lpm flow rate, and the maximum temperature was 230.775 °C and the ΔT was 124.23 °C, which was quite unreasonable, so we stopped these methodologies simulations.

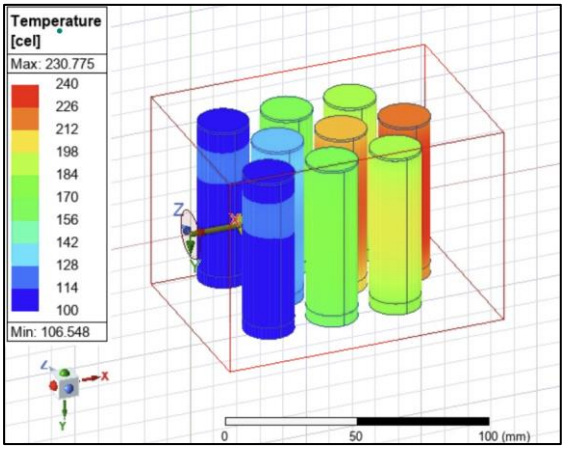

Figure 34. 1 C Discharge Rate at 4 lpm.

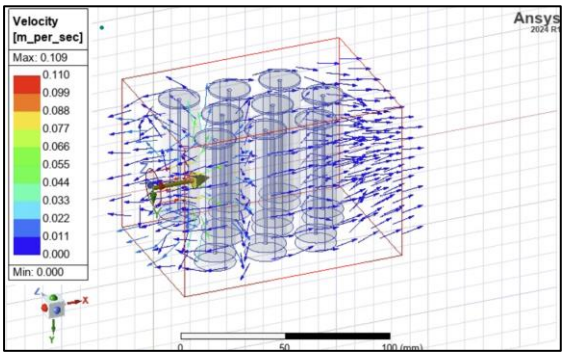

Figure 35. Velocity Vectors at 4 lpm.

Forced Immersion Cooling: The table given is for 3 discharge rates. The table is only for data of 3 discharge rates at 2, 4, 6 lpm respectively.

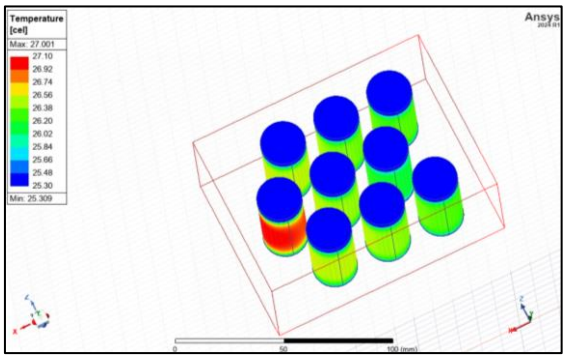

Figure 36. 1 C Discharge Rate 4 lpm.

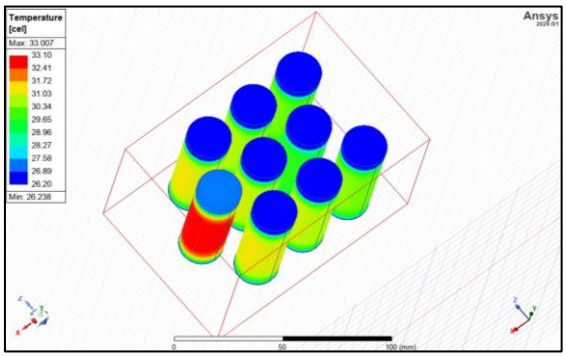

Figure 37. 2 C Discharge Rate 4 lpm.

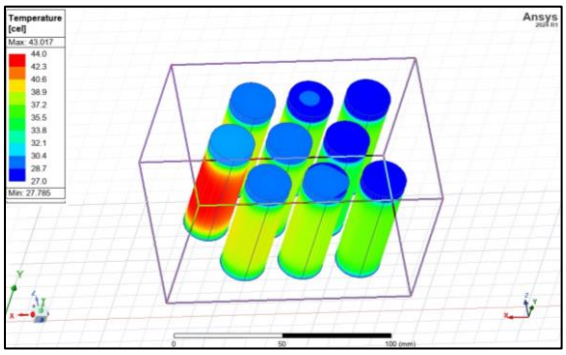

Figure 38. 3 C Discharge Rate 4 lpm.

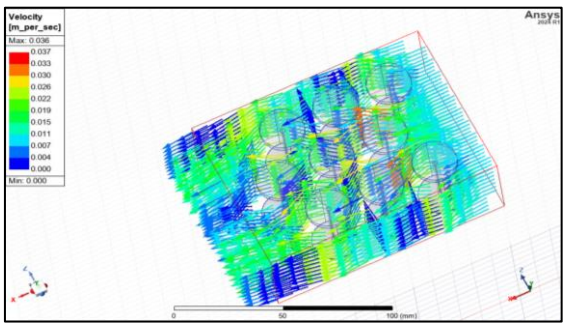

Figure 39. Velocity Vectors at 4 lpm.

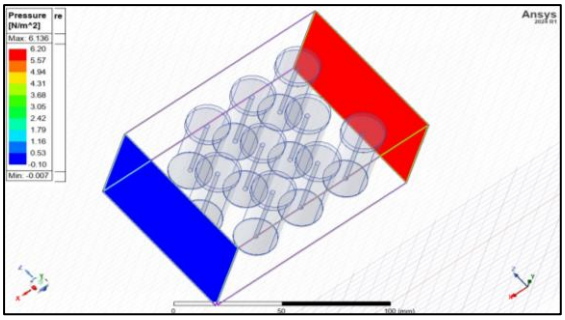

Figure 40. Pressure Plots for 4 lpm.

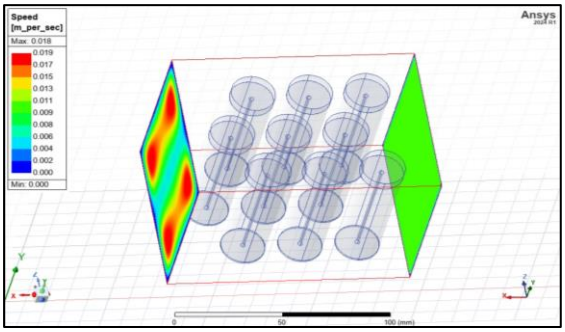

Figure 41. Speed Plots for 4 lpm.

Discharge Rate (C)	Max Temperature (°C)	Del P (N/m^2)	Del T (°C)
1	27.866	2.968	2.436
2	36.473		9.733
3	50.817		21.938
Discharge Rate (C)	Max Temperature (°C)	Del P (N/m^2)	Del T (°C)
1	27.001	6.143	1.692
2	37.007		6.769
3	43.017		15.232
Discharge Rate (C)	Max Temperature (°C)	Del P (N/m^2)	Del T (°C)
1	26.668	9.532	1.425
2	31.752		5.669
3	40.191		12.822

Results and Discussions

The graph demonstrates the thermal performance of various cooling methods as a function of total discharge rate (C). Flow immersion cooling consistently maintains the lowest maximum temperatures across all discharge rates, showing excellent heat dissipation capabilities. For example, at a discharge rate of 3.0 W, the maximum

temperature remains below 100°C for flow immersion, significantly outperforming the other methods. Cold plate cooling also performs well, with relatively moderate temperature rises compared to static immersion and static air, maintaining maximum temperatures below 150°C at the highest discharge rate. In contrast, static immersion cooling shows the steepest temperature increases, reaching temperatures exceeding 500°C at 3.0 W, highlighting its inefficiency in managing high heat loads. Static air cooling lies between cold plate and static immersion performance but still exhibits higher maximum temperatures than flow immersion and cold plate, indicating limited thermal effectiveness for higher discharge rates.

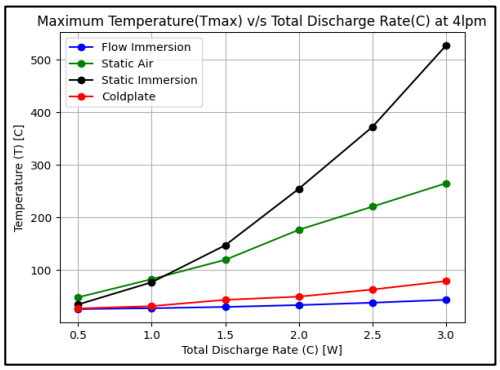

Figure 42. Max Cell Temp v/s Discharge Rate (4 lpm).

The graph highlights the effectiveness of different cooling methods by analyzing the temperature difference (ΔT) versus total discharge rate. Flow immersion cooling demonstrates superior thermal management, maintaining the lowest ΔT values across all discharge rates, with minimal increases even at the highest discharge rate of 3.0 W. This indicates its high efficiency in dissipating heat uniformly. The cold plate also performs effectively, showing moderate increases in ΔT as discharge rates rise, maintaining better thermal performance than static air and static immersion. On the other hand, static air cooling exhibits the steepest rise in ΔT, exceeding 250°C at 3.0 W, which underlines its inadequacy in handling high heat loads. Static immersion cooling similarly underperforms, showing progressively higher ΔT values with increasing discharge rates, indicating limited thermal efficiency for high-power applications. The static air cooling maximum temperature is lesseer than the maximum temperature of static immersion cooling, which is counter-intuitive as there is a three orders of magnitude difference in the thermal diffusivities of mineral oil and air (Thermal diffusivity of air is 1000 times larger than that of mineral oil), and in static cooling, the main form of heat transfer is conduction.

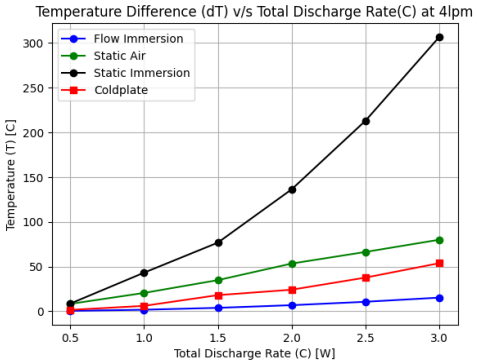

Figure 43. Delta Temp v/s Discharge Rate (4 lpm).

The log-log plot of pressure drop (ΔP) versus flow rate demonstrates significant differences in the hydraulic efficiency of the two cooling systems. The Cold Plate exhibits a steep increase in pressure drop as the flow rate rises, indicating a much higher demand for pumping power. For instance, at a flow rate of 6 lpm, the pressure drop for the Cold Plate is approximately 1000 N/m², highlighting its high hydraulic resistance. In contrast, flow immersion cooling shows a more gradual and linear increase in pressure drop, remaining below 100 N/m² even at the highest flow rate, making it far more energy-efficient in terms of pumping requirements. While the Cold Plate offers effective thermal management, its steep pressure drop curve implies higher operational costs and greater energy demands. This behavior aligns with the Darcy-Weisbach equation, where the head loss due to friction is proportional to the flow velocity squared, emphasizing the need to balance thermal and hydraulic performance in system design.

$$\Delta h = \frac{fLV^2}{2gD}$$

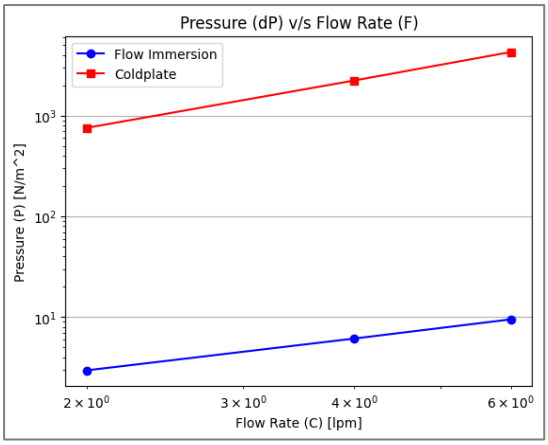

Figure 44. Delta Pressure v/s Flow Rate.

The graph highlights the performance of flow immersion and Cold Plate cooling methods in managing maximum temperature (Tmax) as a function of flow rate at 2.0°C. Flow immersion demonstrates a clear trend of decreasing Tmax with increasing flow rate, improving from approximately 37.5°C at 2 lpm to about 32.5°C at 6 lpm, indicating enhanced cooling efficiency as the flow rate

increases. In contrast, the Cold Plate cooling system maintains a relatively constant Tmax of around 50°C across all flow rates, reflecting limited improvement in thermal performance with increased flow rate. These results suggest that flow immersion cooling is more effective in dissipating heat, particularly at higher flow rates, while the Cold Plate system is less responsive to changes in flow rate, making it less efficient in applications where dynamic thermal management is required.

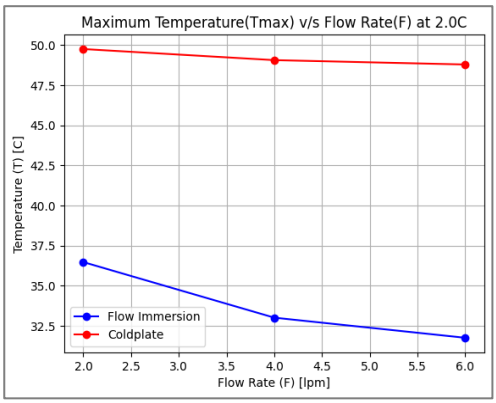

Figure 45. Max Cell Temp v/s Flow Rate.

The graph illustrates the temperature change (ΔT) versus flow rate for flow immersion and Cold Plate cooling systems at 3.0°C. Flow immersion exhibits a decreasing trend in ΔT with increasing flow rate, dropping from around 20°C at 2 lpm to below 15°C at 6 lpm, signifying improved thermal performance at higher flow rates. In contrast, the Cold Plate cooling system maintains a relatively constant and higher ΔT, starting at approximately 60°C at 2 lpm and remaining above 50°C at 6 lpm, indicating limited thermal improvement with increasing flow. These results highlight the superior efficiency of flow immersion cooling in reducing ΔT at higher flow rates, making it better suited for applications requiring dynamic and efficient thermal management. Cold Plate cooling, while functional, appears less responsive to flow rate adjustments, limiting its performance in scenarios with higher heat dissipation demands.

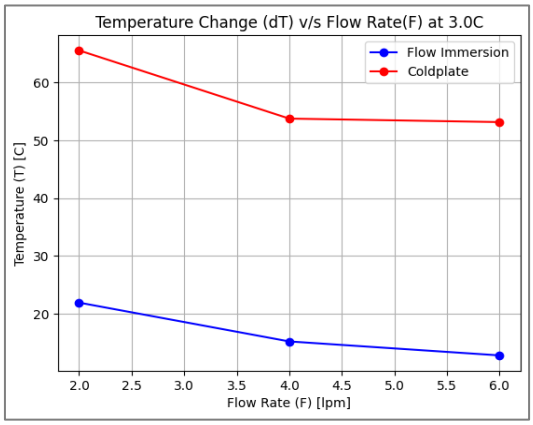

Figure 46. Delta Temp v/s Flow Rate.

Conclusion

From our project work, it can be concluded that flow immersion cooling effectively reduces the maximum battery temperature by 46.23%, maintaining it within the ideal operational range of 15°C to 45°C. Furthermore, temperature fluctuations are significantly minimized, with the variation decreasing from 23.7°C to 7.02°C, ensuring a more stable thermal environment. These improvements directly enhance the performance, safety, and reliability of the battery module. In addition to thermal benefits, flow immersion cooling drastically reduces the pressure drop from 2464 N/m² to 6.21 N/m², leading to improved efficiency and lower energy consumption. This dual advantage of superior thermal regulation and reduced mechanical stress makes flow immersion cooling a highly effective solution for modern EV battery thermal management.

The choice of cooling fluids significantly impacts the performance of the immersion system. Ethylene glycol (50-50) exhibited the best thermal performance, maintaining the lowest maximum cell temperatures among the tested fluids, making it ideal for efficient thermal management. Other fluids, such as toluene, silicone oil, and mineral oil, also provided effective cooling but differed in their thermal conductivity, density, and chemical properties. While mineral oil, often used for its electrical insulation and chemical stability, adds substantial weight to the system, lighter fluids like ethylene glycol and water (in cold plate systems) reduce overall weight, improving vehicle efficiency. Future research could explore optimizing fluid properties to combine thermal performance, chemical stability, and lightweight characteristics for enhanced immersion cooling.

Furthermore, flow immersion cooling allows for a very even temperature distribution and effectively eliminates hot spots within the battery module. In this respect, this technology is superior to air and indirect cooling methods, allowing better longevity, safety, and efficiency of the batteries.

Future Work

The concept of partial immersion cooling offers an intriguing hybrid approach for EV battery thermal management, wherein battery cells are partially submerged in a cooling fluid while the exposed top halves are cooled via airflow. This strategy has the potential to combine the advantages of immersion cooling with the lightweight and simpler design of air-cooled systems. However, the complexity of simulating partial immersion cooling, especially in terms of modeling the interactions between submerged and exposed regions, presents a significant challenge.

Weight optimization remains a crucial consideration for immersion cooling systems. In this study, the enclosure volume required for immersion

cooling was 817.8 cc, with each cell occupying 25.25 cc, resulting in a total of 599.55 cc for nine cells. Using mineral oil for immersion cooling added 0.51 kg per cell, leading to a total system weight exceeding 130 kg for the entire vehicle. In contrast, water was considered in the context of cold plate cooling, where the cooling fluid contributes only 0.054 kg per cell, resulting in a total weight of just over 15 kg, an 88% reduction compared to immersion cooling with mineral oil. Future studies could explore innovative lightweight immersion fluids or hybrid designs that combine the thermal benefits of immersion cooling with the weight advantages of alternative cooling methods. Additionally, advances in enclosure design and material technology could further reduce the overall weight of immersion cooling systems, making them more viable for EV applications where weight is a critical factor.

Acknowledgments

Finally, we would like to thank each member of the team for their immense contribution, and also Professor Winston Zhang and our Teaching Assistant Harsh Tyagi for their continuous guidance and support along the project. It wouldn't have been possible to complete this project without the proper guidance and contribution from all the above mentioned people.

References

[1] Deng, Y., Feng, C., E, J., Zhu, H., Chen, J., Wen, M., & Yin, H. (2018). Effects of different coolants and cooling strategies on the cooling performance of the power lithium-ion battery system: A review. *Applied Thermal Engineering, 142*, 10-29.

[2] Lin, X.-W., Zhou, Z.-F., Yin, J., Zhu, X.-G., Shi, M.-Y., & Chen, B. (2024). A comparative investigation of two-phase immersion thermal management system for lithium-ion battery pack. *Journal of Cleaner Production, 434*, 140472.

[3] Akbarzadeh, M., Kalogiannis, T., Jaguemont, J., Jin, L., Behi, H., Karimi, D., Beheshti, H., Van Mierlo, J., & Berecibar, M. (2021). A comparative study between air cooling and liquid cooling thermal management systems for a high-energy lithium-ion battery module. *Applied Thermal Engineering, 198*, 117503

[4] Lu, Z., Meng, X. Z., Wei, L. C., Hu, W. Y., Zhang, L. Y., & Jin, L. W. (2016). Thermal management of densely-packed EV battery with forced air cooling strategies. *Energy Procedia, 88*, 682-688.

[5] Khalaja, A.H., Halgamugeb, S.K., (2017). A Review on efficient thermal management of air- and liquid-cooled data centers: From chip to the cooling system. Applied Energy 205, 1165-1188

[6] Roe, C., Feng, X., White, G., Li, R., Wang, H., Rui, X., Li, C., Zhang, F., Null, V., Parkes, M., Patel, Y., Wang, Y., Wang, H., Ouyang, M., Offer, G., Wu, B. (2002). Immersion cooling for lithium-ion batteries – A review. Journal of Power Sources 525, 231094

[7] Dubey, P.; Pulugundla, G.; Srouji, A.K. Direct Comparison of Immersion and Cold-Plate based Cooling for Automotive Li-Ion Battery Modules. Energies **2021**, 14,1259.

[8] Oh, I.-T.; Lee, J.-S.; Han, J.-S.; Lee, S.-W.; Kim, S.-J.; Rhi, S.-H. Li-Ion Battery Immersed Heat Pipe Cooling Technology for Electric Vehicles. Electronics **2023**, 12, 4931.

[9] Pesaran, A. A. (2001). Battery thermal management in EVs and HEVs: Issues and solutions. Advanced Automotive Battery Conference, Las Vegas, Nevada.

[10] Xia, G., Cao, L., Bi, G., (2017). A review on battery thermal management in electric vehicle application. Journal of Power Sources 367, 90-105

[11] Zhao, G., Wang, X., Negnevitsky, M., Zhang, H. (2021). A review of air-cooling battery thermal management systems for electric and hybrid electric vehicles. Journal of Power Sources 501, 230001

[12] Al Shdaifat, M. Y., Zulkifli, R., Sopian, K., & Salih, A. A. (2023). A comprehensive review of basics, properties, and thermal issues of EV battery and battery thermal management systems: A comprehensive review. Proceedings of the IMechE Part D: Journal of Automobile Engineering, 237(2-3), 295-311

[13] Clerick, S., Leivens, S., Buytaert, G., & Chore, A. (2022). *Water-based Cooling Fluids to Mitigate the Thermal Management Challenges in New Energy Vehicles*. *ARAI Journal of Mobility Technology*, 2(3), 256-264

[14] Choi, H., Lee, H., Kim, J., & Lee, H. (2023). Hybrid single-phase immersion cooling structure for battery thermal management under fast-charging conditions. Energy Conversion and Management 287, 117053

[15] Hwang, F. S., Confrey, T., Reidy, C., Picovici, D., Callaghan, D., Culliton, D., Nolan, C., (2023). Review of battery thermal management systems in electric vehicles. Renewable and Sustainable Energy Reviews 192, 114171.

[16] Yang Li, Y., Minli Bai, M., Zhou, Z., Wu, W.T., Hu, C., Gao, L., Xinyu Liu, X., Li, Y., Song, Y., (2023). Thermal management for the 18650 lithium-ion battery pack by immersion cooling with fluorinated liquid. Journal of Energy Storage 73, 109166

[17] Chhetri, A., Kashyap, D., Mali, A., Agarwal, C., Ponraj, C., Gobinath, N. (2022). Numerical simulation of the single-phase immersion cooling process using a dielectric fluid in a data server. Materials Today: Proceedings 51, 1532–1538

[18] S. Hemavathi, S., Srinivas, S., Prakash, A.S., (2023). Performance evaluation of a

hydrostatic flow immersion cooling system for high-current discharge Li-ion batteries. Journal of Energy Storage 72, 108560

[19] Jindal, P., Sharma, P., Kundu, M., Singh, S., Shukla, D.K., a, Pawar, V.J.,Wei, Y., Breedon, P.(2022). Computational Fluid Dynamics (CFD) analysis of Graphene Nanoplatelets for the cooling of a multiple-tier Li-ion battery pack. Thermal Science and Engineering Progress 31, 101282

[20] Li, C., Wang, Y., Sun, Z., Wen, X., Wu, J., Feng, L., Wang, Y., Cai, W., Yu, H., Wang, M., Zhu, H., & Liu, D. (2024). Two-phase immersion liquid cooling system for 4680 Li-ion battery thermal management. *Journal of Energy Storage*, *97*, 112952.

[21] Liu, J., Chavan, S., & Kim, S.-C. (2023). Investigation of the electrochemical and thermal characteristics of NCM811-21700 cylindrical lithium-ion battery: A numerical study and model validation. *Energies*, *16*(6407).

[22] Quinn, J. B., Waldmann, T., Richter, K., Kasper, M., & Wohlfahrt-Mehrens, M. (2018). Energy density of cylindrical Li-Ion cells: A comparison of commercial 18650 to the 21700 cells. *Journal of The Electrochemical Society*, *165*(14), A3284–A3291

[23] Saxon, A., Yang, C., Santhanagopalan, S., Keyser, M., & Colclasure, A. (2024). Li-Ion Battery Thermal Characterization for Thermal Management Design. Batteries, 10(4), 136.

[24] Dymyd, L., Ciubotaru, L., Helezen, M., Shah, J. M., Pai, L., Brink, R., Payne, R., Gullbrand, J., & Gore, N. (2020). *Design guidelines for immersion-cooled IT equipment* (Rev. 1.01). Open Compute Project.